

GRADIENT-BASED OPTIMAL CONTROL OF BATTERIES AND HVAC IN DISTRICT ENERGY SYSTEMS

Marco Bonvini¹, Michael Wetter¹

¹Lawrence Berkeley National Laboratory, Berkeley, CA

ABSTRACT

Residential and commercial buildings use nearly 75% of the overall electrical energy in the U.S., and the amount of renewable energy in the grid keeps increasing. Buildings can be an important contributor to ensure a stable grid operation because they can shift their loads to reduce peak demand and flatten the ramps of load increase and decrease. Simulation models that account for building loads and building dynamics, as well as their impact on the electricity distribution grid, are essential to assess different design and control options for buildings and electrical systems. This paper presents the use of such simulation models of dynamic building loads coupled to electrical models within a tool chain that allows efficient numerical solution of nonlinear optimization problems that aim at controlling the voltage stability and thermal comfort while minimizing energy use or energy cost. The optimization problems are formulated using the open-source JModelica software that convert them to a form in which they are solved using the nonlinear programming solver IPOPT. In this formulation, JModelica converts an infinite-dimensional optimization problem, defined on the solution of the differential equations of the simulation model, to a finite-dimensional nonlinear programming problem using computer algebra and collocation methods.

INTRODUCTION

Residential and commercial buildings use nearly 75% of the overall electricity energy in the U.S. The increase of PVs and intermittent loads such as electric vehicles towards a new generation of net zero energy buildings is posing a challenge to the stability of the grid, impacting the reliability of traditional electricity delivery (Ipakchi and Albuyeh, 2009). To avoid problems, efficient transactions between buildings and the grid are needed (Palensky and Dietrich, 2011). Simulation models that account for buildings and their impact on the electricity distribution grid are essential to support the design and operation of the distribution grid (Van Roy et al., 2013). Such multi-disciplinary and multi-domain models have to describe both the interactions and the dynamics affecting these systems. Moreover, once these interactions and dynamics are defined, they should be leveraged to identify optimal control strategies that help stabilizing the grid.

This paper shows how to solve such optimization problems that consider both dynamics and interactions between buildings and the electrical grid. As examples, this paper investigates multiple optimization problems that involve the optimal cooling as well as the charging

and discharging of batteries in a commercial building with and without on-site renewable energy sources. The optimization problems are further extended to investigate the impact that buildings have on the voltage quality in a small neighborhood and how batteries can be controlled to improve it. The models used within the optimization problem have been adapted from the Electrical package (Bonvini et al., 2014) of the Modelica Buildings library (Wetter et al., 2014).

The optimization approach we use differs from other methods in the literature (Guan et al., 2010; Stadler et al., 2009) that use mixed integer linear programming (MILP) techniques. With MILP, it is possible to approximate nonlinearities in the cost function with piecewise linear approximations. The approach we use is based on nonlinear programming (NLP) methods and is able to handle nonlinear dynamics as well as nonlinear constraints on variables of the system. For example, it can be used to minimize the total energy use of a district energy system, or its total electricity costs or CO₂ emissions, while keeping the root mean square (RMS) voltages within the required limits. An other application could be optimal cooling load shift while maintaining thermal comfort within the required limits.

The paper also describes the toolchain based on the open source tool JModelica¹ that allows to reuse simulation models to solve optimization problems. Such a toolchain enables the users to design and operate buildings and the distribution grid more efficiently.

While the examples in this paper use first-principle physical models, the methodology works also with grey box models and with models that are identified from data.

MOTIVATION

Buildings, renewables energy generation plants and distribution grids are engineered systems which are steadily growing in complexity. Modeling and simulation tools are fundamental to support their design and operation. Traditional simulation tools have limited capabilities when it comes to modeling integrated systems. Different legacy tools are available to simulate the various domains (e.g., buildings and electrical grid). However, most building simulation programs such as EnergyPlus (Crawley et al., 2000) do not model the electrical grid, while tools that focus on the electrical distribution grid, such as OpenDSS (Dugan, 2012) and GridLab-D (Chassin et al., 2008) include only simplified building and heating models, or take load curves as input. Hence, if such tools were to

¹See www.jmodelica.org.

be used together, one would require the use of co-simulation (Makhmalbaf et al., 2014; Chatzivasileiadis et al., 2015). An example of building simulation program that allows to model electrical models is ESP-r (Eng, 1998).

Solving design optimization or optimal control problems with many decision variables is difficult if evaluating the cost or constraint functions requires co-simulation of legacy code. The reason is that solving large optimization problems is most efficient if first or second order derivatives of the cost and constraint functions with respect to the design parameters exist and are accessible. However, legacy code is often written in such a way that state trajectories are not differentiable with respect to the independent parameters. Moreover, in the cases where gradients exist, legacy tools often do not make them accessible, thereby requiring the optimization algorithm to compute numerical approximations of the gradient. This is computationally costly and leads to more complex algorithms (Polak, 1997). Furthermore, optimization algorithms have been shown to fail to converge if the cost function is discontinuous, as identified in Energy-Plus (Wetter and Wright, 2004).

The increased integration of building and district energy systems leads to complex dynamic systems that require new approaches for design and operational optimization. The Modelica Buildings library (Wetter et al., 2014) and the IDEAS library (Van Roy et al., 2013) are examples of modeling libraries that have been used to overcome the aforementioned limitations. These libraries are based on Modelica, an equation-based modeling language for dynamic, multi-physics engineered systems (Mattsson et al., 1998). As Modelica is a declarative language, models expressed in this language can be symbolically analyzed and manipulated to bring them in a form that is more amenable for simulation and optimization. Therefore, Modelica is well suited to express models for large scale optimization (Åkesson et al., 2010). Figure 1 shows the information flow for equation-based models when used to solve optimization problems. The engineers and designers simulate models to investigate the behavior of the system for different design alternatives. To solve an optimal control problem, the models are augmented by adding objective and constraint functions. Next, the models are symbolically manipulated using computer algebra to bring the optimization problem into a form that allows an efficient computation of the optimal control function. The optimal control signal is then sent to the building system. Using measured data, models can be adapted and current values of observable states can be estimated to align the states of the models with the states of the building system.

Such an approach can be done using the open source tool JModelica (Åkesson et al., 2009) which we used in our experiments for this paper. JModelica uses the equation-based structure of the model to con-

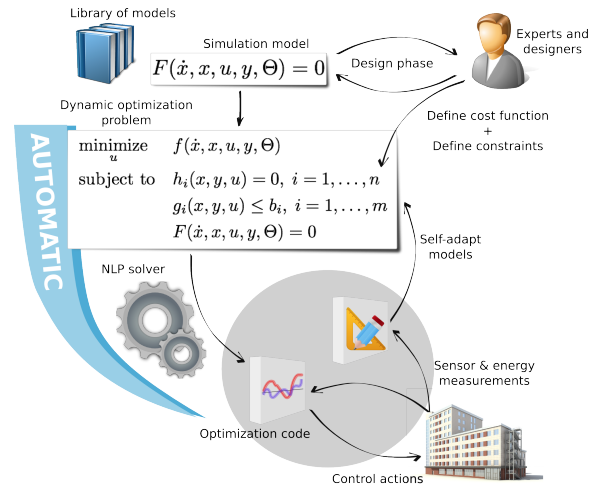


Figure 1: Model-based optimization toolchain based on JModelica.

vert an infinite-dimensional optimization problem into a finite-dimensional nonlinear programming problem that is then solved using a nonlinear solver (e.g., IPOPT). The following sections provide an overview of the systems that can be used with JModelica and the methods that automatically generate an optimization problem starting from a simulation model, constraints and an objective function.

METHODOLOGY

The systems considered in this paper can be described by a system of differential algebraic equations (DAE) of index less or equal to one. The general form is

$$F(t, \dot{x}(t), x(t), u(t), y(t), \Theta) = 0, \quad (1)$$

where $t \in [t_0, t_f]$ is time for some initial and final time t_0 and t_f , $x(t) \in \mathbb{R}^{n_x}$ is the state vector, $u(t) \in \mathbb{R}^{n_u}$ is the input vector, $y(t) \in \mathbb{R}^{n_y}$ is the vector of algebraic variables, and $\Theta \in \mathbb{R}^p$ is the vector of parameters. The initial conditions for (1) can be implicitly specified as

$$F_0(\dot{x}(t_0), x(t_0), u(t_0), y(t_0), \Theta) = 0. \quad (2)$$

A comprehensive description of the generalized optimization problems that can be solved with JModelica is

$$\begin{aligned} & \text{minimize} && f(t, z(t), \Theta) && (3a) \\ & z(\cdot) \in \mathcal{Z}, \Theta \in \mathbb{R}^p \end{aligned}$$

$$\text{subject to} \quad F(t, z(t), \Theta) = 0, \quad (3b)$$

$$F_0(z(t_0), \Theta) = 0, \quad (3c)$$

$$z_L \leq z(t) \leq z_U, \quad (3d)$$

$$p_L \leq \Theta \leq p_U, \quad (3e)$$

$$h(t, z(t), \Theta) = 0, \quad (3f)$$

$$g(t, z(t), \Theta) \leq 0, \quad (3g)$$

$$H(t, Z_h, \Theta) = 0, \quad (3h)$$

$$G(t, Z_g, \Theta) \leq 0, \quad (3i)$$

$$\forall t \in [t_0, t_f],$$

where $z(\cdot) = [x(\cdot), y(\cdot), u(\cdot)]$, $f(\cdot, \cdot, \cdot) : \mathbb{R} \times \mathbb{R}^{n_x+n_y+n_u} \times \mathbb{R}^p \rightarrow \mathbb{R}$ is the cost function, the equalities (3b) and (3c) describe the dynamics of the system and its initial conditions, (3d) and (3e) define the upper and lower bounds for the time dependent variables and the parameters, (3f) and (3g) are equality and inequality path constraints, (3h) and (3i) are the equality and inequality point constraints, where Z_h and Z_e are the points where these constraints are imposed. To establish second order optimality conditions and to find a first order optimal solution, for (3) the functions $f(\cdot, \cdot, \cdot)$, $F(\cdot, \cdot, \cdot)$ and $F_0(\cdot, \cdot)$ have to be twice continuously differentiable.

The general optimization problem (3) covers a large class of problems, that include optimal set point tracking, and parameter calibration. The problem is infinite dimensional because the optimal solution $z(\cdot)$ is a functional in the set of admissible trajectories \mathcal{Z} . The techniques and methods described by Biegler (2010) allows to convert an infinite dimensional optimization problem of the form (3) to a finite dimensional nonlinear programming problem of the form

$$\begin{aligned} & \underset{w \in \mathbb{R}^{n_w}}{\text{minimize}} && f(w), \\ & \text{subject to} && w_L \leq w \leq w_U, \\ & && g(w) = 0, \\ & && h(w) \leq 0, \end{aligned} \quad (4)$$

where $w \in \mathbb{R}^{n_w}$ is a finite dimensional variable. JModelica uses the direct collocation method to convert the infinite dimensional problem (3) into its equivalent finite dimensional form (4). The method uses polynomials defined over a finite number of support points, the so-called collocation points, to approximate the trajectories of the dynamic system. Before assigning the collocation points, the time horizon $[t_0, t_f]$ is divided into n_e elements. Next, within each element, the time-dependent variable $z(t)$ is approximated using a vector valued polynomial $z_i(t) = (\hat{x}_i(t), x_i(t), u_i(t), y_i(t))$. The collocation polynomials are formed by choosing a number of collocation points n_c , within each of the n_e elements. The number of collocation points n_c is assumed to be the same for each element. The collocation polynomials are created using Lagrange interpolating polynomials that use the collocation points as interpolation points. The collocation points are selected using the Radau collocation method, which place a collocation point at the end of each element and then select the others to maximize accuracy. In addition to the collocation points, the start point of every element is added to impose constraints on the continuity of the state trajectories between different elements. The collocation polynomials that ap-

proximate $z(t)$ in the element i are

$$x_i(\tau) = \sum_{k=0}^{n_c} x_{i,k} \tilde{l}_k(\tau), \quad (5a)$$

$$u_i(\tau) = \sum_{k=1}^{n_c} u_{i,k} l_k(\tau), \quad (5b)$$

$$y_i(\tau) = \sum_{k=1}^{n_c} y_{i,k} l_k(\tau), \quad (5c)$$

where $\tau \in [0, 1]$ is the normalized time in each element $i \in \{1, \dots, n_e\}$, $l_k(\tau)$ is the Lagrange basis polynomial and $\tilde{l}_k(\tau)$ is the Lagrange basis polynomial that includes the first point to ensure continuity of the state trajectories. Since the time is normalized in all the elements, the basis polynomials are the same for every element. The polynomial approximation of the derivative $\dot{x}_i(\tau)$ is the derivative of (5a). The infinite dimensional optimization problem (3) is converted into a finite dimensional problem that can be solved using a NLP solver. The conversion is done by replacing the continuous variables $z(t)$ and t with their discretized versions, $z_i(t)$ and t_i . For a more detailed overview see Magnusson and Åkesson (2012).

EXAMPLE

We present a series of examples that investigate the optimal cooling, charge and discharge of batteries in a neighborhood with commercial buildings and on-site renewable energy sources. The series starts with the optimization of a single building. Next, we increase complexity by adding more buildings, PVs and batteries. The series concludes with an optimization problem where batteries in different buildings are coordinated to improve the voltage quality of the neighborhood while satisfying thermal comfort constraints.

BUILDING MODEL

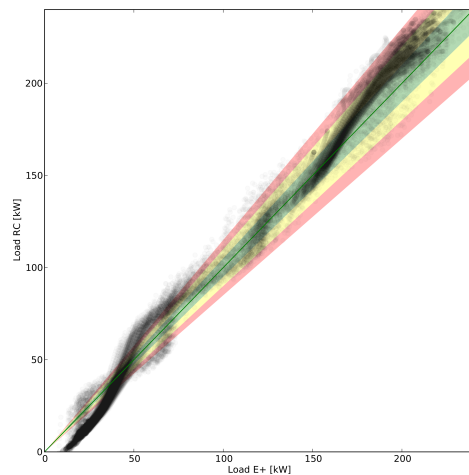


Figure 2: Comparison of cooling load computed by a reduced order model and the original EnergyPlus model. The green, yellow and red colored area represent a relative error of 5%, 10% and 15%.

The building model used in the example is a 54,000 ft² two story steel-frame office and laboratory building, located in Berkeley, CA. An EnergyPlus model of the building was available, which we converted to an equivalent resistor-capacitor (RC) model using the Building Resistance-Capacitance Modeling (BRCM) toolbox (Sturzenegger et al., 2014). The linear RC model constitutes a simplification of the whole-building EnergyPlus model. The number of outputs of the building model has been limited to the average return air temperatures $T_R(t)$ of the thermal zones. The model is

$$\dot{x}(t) = Ax(t) + B_v v(t), \quad (6a)$$

$$y(t) = Cx(t), \quad (6b)$$

$$C = \left[\frac{V_1}{V_{tot}}, \dots, \frac{V_{n_z}}{V_{tot}}, 0, \dots, 0 \right],$$

where $x(t) \in \mathbb{R}^{n_x}$ is the state vector containing all the temperatures of the zones, internal masses and wall layers, $v(t) \in \mathbb{R}^{n_v}$ are the predicted disturbances (such as external air temperature, solar radiation and internal heat gains), $y(t) \in \mathbb{R}^{n_y}$, with $n_y = 1$, is the return air temperature, $C \in \mathbb{R} \times \mathbb{R}^{n_x}$ is the output matrix, n_z is the number of thermal zones (the first n_z elements of the state vector $x(t)$), V_i for $i \in \{1, \dots, n_z\}$ is the volume of the i -th thermal zone, and $V_{tot} = \sum_{i=1}^{n_z} V_i$ is the sum of all the volumes. The vector of known disturbances $v(t)$ and outputs $y(t)$ are defined as

$$v(t) = [Q_{ihg}(t), T_{amb}(t), T_{gnd}(t), S_e(t), S_w(t), S_n(t), S_s(t)]^T,$$

$$y(t) = [T_R(t)],$$

where $Q_{ihg}(t)$ is the internal heat gain, $T_{amb}(t)$ is the outside air temperature, $T_{gnd}(t)$ is the ground temperature and $S_i(t)$, with $i \in \{n, s, w, e\}$, are the global direct plus the diffuse solar radiation on the north, south, west and east directions. For this study, we further reduce the size of the initial RC model using a method that eliminates the state variables characterized by the smallest Henkel singular values (Glover, 1984). With such a method we reduced the number of states of the initial RC model from 106 to 8 state variables. Figure 2 shows a comparison between the cooling load predicted by the reduced order model with respect to the original EnergyPlus model over the summer period. The higher relative errors that occur in the lower left corner are due to the presence of nonlinear effects such as radiation to the sky during night time. The HVAC model provides a simple description of the overall performance of the cooling system and is described by the following equations

$$COP(t) = f(T_{amb}(t)), \quad (8a)$$

$$Q_{ihg}(t) = P_o(t) + P_l(t) + P_p(t) + P_{cool}(t), \quad (8b)$$

$$P_{el}(t) = P_l(t) + P_p(t) + \frac{P_{cool}(t)}{COP(t)}, \quad (8c)$$

where we used for the coefficient of performance $COP(t)$ a linear function of the outside air temperature, $P_o(t)$, $P_l(t)$ and $P_p(t)$ are the internal heat gains due to occupants, lights and plug loads, $P_{el}(t)$ is the electrical power consumption of the building and HVAC system and $P_{cool}(t)$ is the cooling power that is needed to maintain the thermal comfort inside the building. $P_{cool}(t)$ is also one of the decision variables of the optimization problem.

ELECTRIC MODELS

In the electrical domain, the building is represented by an inductive load with PVs and a battery connected to it. The electric models use the quasi-stationary phasorial representation, i.e. voltages and currents sinusoids have no transients and thus can be represented by vectors in the complex plane. The apparent power of the inductive load representing the building is

$$S_{bui}(t) = P_{el}(t)(1 + j \tan \phi), \quad (9)$$

where ϕ is the phase shift between the voltage and current phasors. If $\phi > 0$, the load is inductive. The model of the battery is

$$E_{batt} \frac{d}{dt} SOC(t) = P_{batt}(t), \quad (10)$$

where E_{batt} is the storage capacity of the battery, $SOC(t)$ is the state of charge and $P_{batt}(t)$ is the power stored into or drawn from the battery. $P_{batt}(t)$ is the second decision variable of the optimization problem. The battery is connected to a DC/AC converter and we assume that this conversion does not introduce reactive power. The PV model is

$$P_{pv}(t) = (S_e(t)A_e + S_w(t)A_w + S_n(t)A_n + S_s(t)A_s) \eta_{PV}, \quad (11a)$$

where $P_{pv}(t)$ is the power produced by the PVs, A_e , A_w , A_n , and A_s are the areas of the PVs panels oriented towards east, west, south and north, and η_{PV} is a parameter that accounts for the efficiency of the PV modules and the efficiency of the inverter. The reactive power generated by the DC/AC converter connected to the PV is assumed to be equal to zero.

The quasi-stationary assumption allows to model the electric loads, PVs, and lines with algebraic equations that are coupled to the differential equations of the buildings and electric storages. Such representation helps the collocation method because it does not have to approximate on the same time grid both fast electrical transients and slow thermal dynamics.

CONSTRAINTS AND COST FUNCTIONS

All the optimization problems either minimize the energy used by the building $E(\cdot, \cdot) : \mathbb{R} \times \mathbb{R} \rightarrow \mathbb{R}$ or the energy cost $M(\cdot, \cdot) : \mathbb{R} \times \mathbb{R} \rightarrow \mathbb{R}$. The cost functions

are defined over a period of five days as

$$E(t_0, t_f) = \int_{t_0}^{t_f} \max(0, P_{el}(t) + P_{batt}(t) + P_{pv}(t))dt, \quad (12a)$$

$$M(t_0, t_f) = \int_{t_0}^{t_f} p(t)(P_{el}(t) + P_{batt}(t) + P_{pv}(t))dt, \quad (12b)$$

where $p(t)$ is the time-varying price signal, t_0 and t_f are the initial and final times of the optimization period. The price is assumed to be the same for either buying or selling energy and it varies between 0.11\$/kWh and 0.24\$/kWh. Note that the $\max(\cdot, \cdot)$ function, implemented using a smooth approximation, incentivizes each building to use its electric or thermal energy storage. The reason is that feeding power to the grid does not decrease the cost function $E(t_0, t_f)$, therefore it disincentives the building from feeding power back to the grid reducing possible overvoltages. Later in this paper, we will impose inequality constraints on the maximum voltage. The constraints included in the optimization problem define both the thermal comfort requirements as well the limits of operation of the electric storage and the HVAC system. The constraints are

$$P_{batt}^{max} \leq P_{batt}(t) \leq P_{batt}^{max}, \quad (13a)$$

$$P_{cool}^{max} \leq P_{cool}(t) \leq 0, \quad (13b)$$

$$T_R^{min} \leq T_R(t) \leq T_R^{max}, \quad (13c)$$

$$SOC^{min} \leq SOC(t) \leq SOC^{max}, \quad (13d)$$

where P_{batt}^{max} and P_{batt}^{max} are the maximum discharging and charging power of the battery, P_{cool}^{max} is the maximum cooling capacity of the HVAC system, T_R^{min} and T_R^{max} are the comfort constraints on the return air temperatures and SOC^{min} and SOC^{max} are the allowed minimum and maximum charge of the battery.

We initialized all the optimization problems using a solution based on a relay controller that keeps the return air temperature $T_R(t)$ within the limits specified by (13). Such sub-optimal and feasible initial solution helps the nonlinear solver to find the optimal trajectory.

SCENARIO 1

In this scenario, the building has neither PVs nor a battery. The cooling power profiles are computed in order to minimize either the energy use or the energy cost. Figure 3 shows the results of the optimization. When the controller minimizes energy use $E(t_0, t_f)$, the room temperature is always at the higher limit of the comfort range (the red line). When minimizing energy cost $M(t_0, t_f)$, because of the higher price during the day, the controller shifts the cooling load to the night and causes the building to pre-cool (black line).

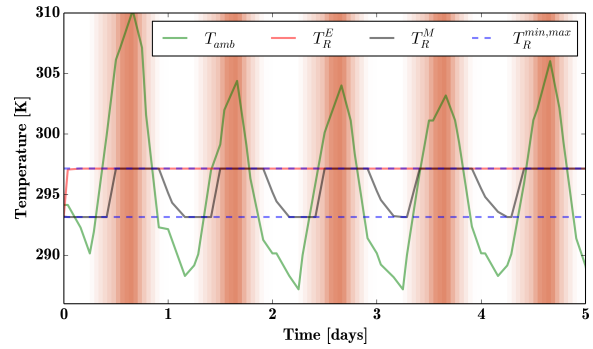


Figure 3: Scenario 1 – The figure shows the temperature in the building when controlled to minimize energy (red line) and to minimize cost (black line). The outside air temperature and the comfort temperature range are shown in green and dashed blue lines. The darker the background color, the higher the energy price.

SCENARIO 2

In this scenario the building has PVs but no battery. As in scenario 1, the only degree of freedom for the controller is to decide the optimal allocation of the cooling power. Figure 4 shows the results for minimizing energy or cost. When minimizing energy use, the controller decides to use the power provided by the PVs to cool the building during the day (red line) as feeding electricity to the grid does not reduce the objective function $E(t_0, t_f)$. However, when minimizing the energy cost $M(t_0, t_f)$, the controller, as in scenario 1, shifts the cooling to the night and pre-cools the building (black line).

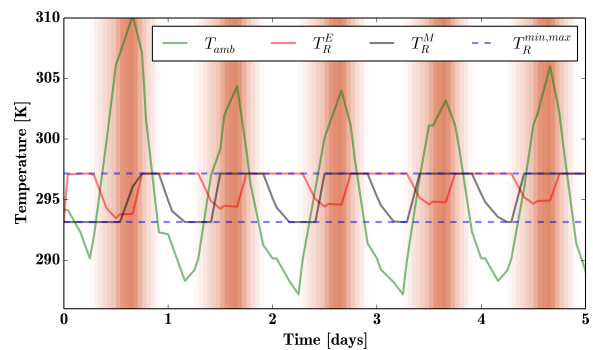


Figure 4: Scenario 2 – The figure shows the temperature in the building when controlled to minimize energy (red line) and to minimize cost (black line). The outside air temperature and the comfort temperature range are shown in green and dashed blue lines. The darker the background color, the higher the energy price.

SCENARIO 3

In the third scenario we add a battery to the system, thus the optimization problem has an extra degree of freedom with respect to scenario 2. In this case, the controller can decide the optimal cooling power deliv-

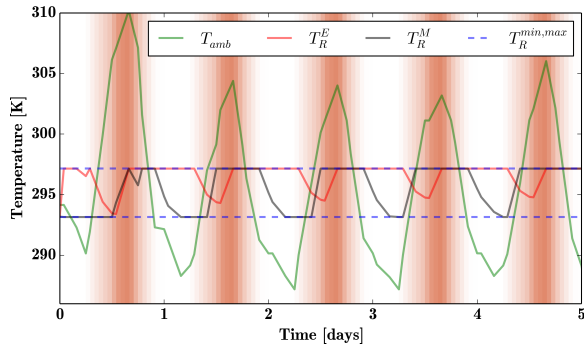


Figure 5: Scenario 3 – The figure shows the temperature in the building when controlled while minimizing the energy (red line) and while minimizing the cost (black line). The outside air temperature and the comfort temperature range (green and dashed blue lines). The darker the background color, the higher the energy price.

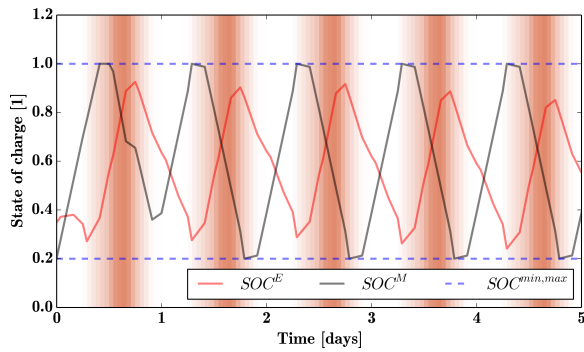


Figure 6: Scenario 3 – The figure shows the temperature in the building when controlled to minimize energy (red line) and to minimize cost (black line). The outside air temperature and the comfort temperature range are shown in green and dashed blue lines. The darker the background color, the higher the energy price.

ery as well the optimal charge and discharge schedule of the battery. Figures 5 and 6 show the results of this scenario. Compared to scenario 2, when minimizing energy, the temperature of the building decreases less since part of the power produced by the PVs is stored in the batteries and then used during nighttime when the COP is higher and the PVs do not generate power. When optimizing the cost of energy, the variability of the energy price and the thermal constraints play a dominant role. The controller pre-cools the building as much as possible when the energy is cheap in order to minimize the electricity cost during the high-price period. Figure 6 shows how the extra degree of freedom provided by the battery is utilized. The controller that minimizes the energy use $E(t_0, t_f)$ charges the battery during the day when the PVs are producing power (red line). The controller that minimizing the cost of energy $M(t_0, t_f)$ charges the battery at night using cheap energy and discharges the battery during

the day (black line). It turns out that the controller that minimizes energy does not fully charge and discharge the battery. In contrast, the controller that minimizes the cost of energy stores as much energy as possible when it is cheap and then uses it during the peak time.

SCENARIO 4

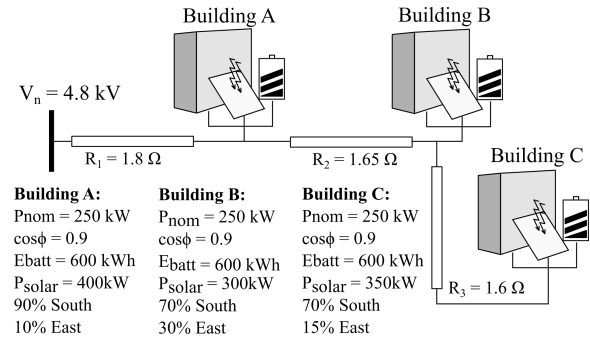


Figure 7: Schematic representation of the neighborhood.

In this scenario, we consider three buildings. The models used in the former scenario have been parametrized with different values to represent three commercial buildings as shown in Figure 7. The parameters that have been modified are the distribution of the PVs along the different directions, and the nominal power of the PVs of each building. This change causes diversity on the magnitude and shape of the generated power among the buildings. In this scenario, we also consider the grid voltage, and one optimization scenario includes inequality constraints on the RMS voltage at the building to grid connections. For every building, the constraints defined in (13) are still applied, and additional constraints are

$$V_A^{rms}(t) \leq V^{max}, \quad (14a)$$

$$V_B^{rms}(t) \leq V^{max}, \quad (14b)$$

$$V_C^{rms}(t) \leq V^{max}, \quad (14c)$$

where $V_A^{rms}(t)$, $V_B^{rms}(t)$ and $V_C^{rms}(t)$ are the RMS voltages of the buildings, $V^{max} = 1.02 V_n$ is the maximum allowed voltage, and V_n is the nominal voltage of the network. It is important to note that the voltage constraints (14) are nonlinear since the RMS voltage is defined as

$$V^{rms}(t) = \sqrt{V_{Re}(t)^2 + V_{Im}(t)^2}, \quad (15)$$

where $V_{Re}(t)$ and $V_{Im}(t)$ are the real and imaginary components of the voltage phasors.

Figure 8 shows the voltage variations in the different nodes of the neighborhood under the optimal control function of scenario 3. The blue lines show the voltages when the cost function of the optimization is the energy used $E(t_0, t_f)$. In this case, the voltages do not reach the red shaded area that corresponds to a RMS voltage that is 2% higher than the nominal

value of $V_n = 4.8$ kW. Overvoltages happen when the buildings are controlled to minimize the cost of energy $M(t_0, t_f)$ (red lines). This happens because the buildings charge their batteries during the night and sell the power generated by the PVs during the day. The green lines in Figure 8 show the results of the new optimization problem that also takes into account the voltage constraints (14).

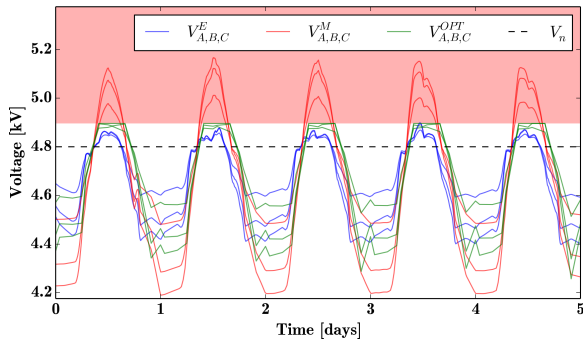


Figure 8: RMS voltages of the buildings A, B and C. The blue lines are the voltages when the buildings are individually controlled to minimize the energy use, the red lines when they are individually controlled to minimize their energy cost, and the green lines when all the buildings are controlled to minimize energy cost while satisfying thermal and voltage constraints. The red shaded area indicates the voltage violation region.

RESULTS AND DISCUSSION

Table 1 compares the results of scenario 1, 2 and 3. As expected, when PVs and batteries are added, the value of the cost function is reduced. An interesting fact happens when transitioning from PVs only to PVs and battery, i.e., from scenario 2 to 3. For example when minimizing with respect to the cost of energy $M(t_0, t_f)$, the energy use $E(t_0, t_f)$ increases despite the lower cost. The same is true when optimizing with respect to the energy use $E(t_0, t_f)$: the energy use is less but its cost is higher.

Table 1: Comparison of total energy use and cost of energy in the different cases. Opt. M are results when minimizing the cost of energy $M(t_0, t_f)$ and Opt. E are the results when minimizing energy cost from the grid $E(t_0, t_f)$.

Scenario	Energy [kWh]		Cost [\$]	
	Opt. E	Opt. M	Opt. E.	Opt. M.
1	25.7	26.0	3978	3948
2	11.8	13.0	810	684
3	9.7	15.3	913	420

When taking into account the whole neighborhood, the optimization strategy that minimizes the energy used from the grid keeps voltage levels low since each building tries to use as much power produced by the PVs as possible. Hence, this strategy attenuates the chances of over voltages in the network. Optimizing the cost of energy introduces high grid voltages

as the buildings try to reduce their energy use during peak time and selling as much solar power as possible. A coordinated action, obtained by solving an optimization problem with both, thermal and voltage constraints, solve this issue. However, the cost of this voltage-aware control action impacts the total cost of operation. The economic impact affects in particular the buildings that are more distant from the source, increasing the cost of energy up to 17% for building C while only 12% for building B.

This optimization scenario includes six independent functions to be varied, which are the cooling power of the buildings and the charge or discharge power of the batteries. The total number of variables of the finite-dimensional optimization problem solved by IPOPT depends on the number of elements n_e and collocation points n_c . Different number of elements have been used to evaluate the performances of the optimization method. The number of collocation points in each element has been kept constant $n_c = 3$. Table 2 shows the results of the analysis. The optimization problems have been solved on a Linux virtual machine with 2GB of memory and 4 cores, using Virtual Box as virtual machine manager. The host machine is a MacBook Pro with a 3 GHz Intel Core i7 processor and 16 GB of memory. Despite the number of variables of the finite-dimensional optimization problem, the number of iterations and the time needed to converge to an optimal solution indicate that the use of gradient based methods are an efficient way to handle such optimization problems.

Table 2: Performances of the optimization method in scenario 4 using different number of elements n_e .

n_e	Variables	Iterations	Time [s]
24	14094	136	23.88
48	28038	253	56.72
96	55926	443	1164.74

CONCLUSIONS

This paper demonstrated how simulation models can be reused to generate optimization problems using a toolchain that leverages the Modelica modeling language and nonlinear programming algorithms. Models adapted from the Modelica Buildings library have been used in conjunction with JModelica that solved the optimization problems. The example demonstrated how different optimization problems can be created by incrementally increasing the complexity of the model. The example also demonstrated how nonlinear optimization problems that involve both thermal and electrical domains in presence of nonlinear cost and constraint functions can be solved. The performances of the optimization method have been tested by dividing the optimization interval with different number of elements. The results show that gradient-based methods are efficient in solving optimal control problems for building and grid integration with large number of

variables.

ACKNOWLEDGEMENT

This research was supported by the Assistant Secretary for Energy Efficiency and Renewable Energy, Office of Building Technologies of the U.S. Department of Energy, under Contract No. DE-AC02-05CH11231. This work emerged from the Annex 60 project, an international project conducted under the umbrella of the International Energy Agency (IEA) within the Energy in Buildings and Communities (EBC) Programme. Annex 60 will develop and demonstrate new generation computational tools for building and community energy systems based on Modelica, Functional Mockup Interface and BIM standards.

REFERENCES

- Åkesson, J., Årzén, K.-E., Gäfvert, M., Bergdahl, T., and Tummescheit, H. 2010. Modeling and optimization with optimica and jmodelica. orglanguages and tools for solving large-scale dynamic optimization problems. *Computers & Chemical Engineering*, 34(11):1737–1749.
- Åkesson, J., Gäfvert, M., and Tummescheit, H. 2009. Jmodelica—an open source platform for optimization of modelica models. In *6th Vienna International Conference on Mathematical Modelling*.
- Biegler, L. T. 2010. *Nonlinear programming: concepts, algorithms, and applications to chemical processes*, volume 10. SIAM.
- Bonvini, M., Wetter, M., and Noudui, T. S. 2014. A modelica package for buildings-to-electrical grid integration. In *Proc. of Fifth German-Austrian IBPSA Conference*, volume 1, pages 6–13, Aachen, Germany. BauSIM.
- Chassin, D., Schneider, K., and Gerkenmeyer, C. 2008. Gridlab-d: An open-source power systems modeling and simulation environment. In *Transmission and Distribution Conference and Exposition, 2008. T&D 2008; D. IEEE/PES*, pages 1–5. IEEE.
- Chatzivasileiadis, S., Bonvini, M., Matanza, J., Yin, R., Liu, Z., Noudui, T., Kara, E. C., Parmar, R., Lorenzetti, D., Wetter, M., and Kiliccote, S. 2015. Cyber physical modeling of distributed resources for distribution system operations. *ArXiv e-prints*.
- Crawley, D. B., Lawrie, L. K., Pedersen, C. O., and Winkelmann, F. C. 2000. Energy plus: energy simulation program. *ASHRAE journal*, 42(4):49–56.
- Dugan, R. C. 2012. Reference guide: The open distribution system simulator (openss). *Electric Power Research Institute, Inc.*
- Eng, N. J. K. B. 1998. Towards a design environment for building-integrated energy systems: the integration of electrical power flow modelling with building simulation.
- Glover, K. 1984. All optimal Hankel-norm approximations of linear multivariable systems and their L-inf error bounds. *International Journal of Control*, 39(6):1115–1193.
- Guan, X., Xu, Z., and Jia, Q.-S. 2010. Energy-efficient buildings facilitated by microgrid. *Smart Grid, IEEE Transactions on*, 1(3):243–252.
- Ipakchi, A. and Albuyeh, F. 2009. Grid of the future. *Power and Energy Magazine, IEEE*, 7(2):52–62.
- Magnusson, F. and Åkesson, J. 2012. Collocation methods for optimization in a modelica environment. In *9th International Modelica Conference*.
- Makhmalbaf, A., Fuller, J., Srivastava, V., Ciraci, S., and Daily, J. 2014. Co-simulation of detailed whole building with the power system to study smart grid applications. In *Technologies for Sustainability (SusTech), 2014 IEEE Conference on*, pages 192–198.
- Mattsson, S. E., Elmqvist, H., and Otter, M. 1998. Physical system modeling with modelica. *Control Engineering Practice*, 6(4):501–510.
- Palensky, P. and Dietrich, D. 2011. Demand side management: Demand response, intelligent energy systems, and smart loads. *Industrial Informatics, IEEE Transactions on*, 7(3):381–388.
- Polak, E. 1997. *Optimization, Algorithms and Consistent Approximations*, volume 124 of *Applied Mathematical Sciences*. Springer Verlag.
- Stadler, M., Marnay, C., Siddiqui, A., Lai, J., and Aki, H. 2009. Integrated building energy systems design considering storage technologies. Technical report, Ernest Orlando Lawrence Berkeley National Laboratory, Berkeley, CA (United States). Funding organisation: Environmental Energy Technologies Division (United States).
- Sturzenegger, D., Gyalistras, D., Semeraro, V., Morari, M., and Smith, R. 2014. BRCM Matlab toolbox: Model generation for model predictive building control. In *American Control Conference 2014*, pages 1–5.
- Van Roy, J., Verbruggen, B., and Driesen, J. 2013. Ideas for tomorrow. *IEEE Power & Energy Magazine*, 11(5):75–81.
- Wetter, M. and Wright, J. 2004. A comparison of deterministic and probabilistic optimization algorithms for nonsmooth simulation-based optimization. *Building and Environment*, 39(8):989–999.
- Wetter, M., Zuo, W., Noudui, T. S., and Pang, X. 2014. Modelica Buildings library. *Journal of Building Performance Simulation*, 7(4):253–270.